ACS OMEGA

http://pubs.acs.org/journal/acsodf

Article

Developing Biodegradable Nanoparticles Loaded with Mometasone Furoate for Potential Nasal Drug Delivery

Jumana Far, Muhammad Abdel-Haq, Maayan Gruber, and Aiman Abu Ammar*

Cite This: *ACS Omega* 2020, 5, 7432–7439

Read Online

ACCESS | Metrics & More | Article Recommendations | Supporting Information

ABSTRACT: Intranasal drug administration is considered a routine in the treatment of many nasal conditions including chronic rhinosinusitis (CRS), which is a common disease involving long-term inflammation of the nasal mucosa. Topical nasal steroid treatment is safe and easy to use and plays a basic role in both nonsurgical and surgical treatments for CRS. Intranasal steroid therapy for various time intervals is commonly used before and after endoscopic CRS nasal surgeries to reduce inflammation and edema and to improve mucosal healing. The medication is currently administered via conventional nasal sprays; therefore, there is an incentive to develop more efficient drug delivery systems for the controlled release of topical steroids into the sinonasal cavities over a prolonged period of time. In this study, poly(lactic-*co*-glycolic acid) (PLGA) nanoparticles (NPs) loaded with mometasone furoate (MF) were generated using the nanoprecipitation method and characterized physicochemically and morphologically. MF NPs exhibited adequate physicochemical properties and high drug encapsulation efficiency and loading content. MF exhibited sustained release from NPs over 7 days in vitro with an initial burst release; various mathematical models were applied to determine the kinetics of drug release. Having demonstrated the ability to load MF in PLGA-NPs using the nanoprecipitation method for the first time, these NPs urge the need for additional investigations to demonstrate their therapeutic potential in nasal delivery applications.

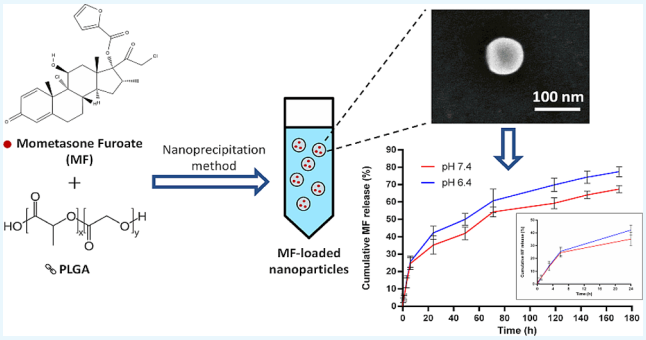

1. INTRODUCTION

Chronic rhinosinusitis (CRS) is a prevalent inflammatory disease affecting the nasal cavity and the paranasal sinuses, which can significantly affect a person's daily functioning and quality of life. It is generally characterized by nasal congestion and discharge lasting at least 12 weeks.[1] The therapeutic approach for patients with CRS involves complex combinations of surgical and medical therapies, while the use of topical and systemic steroids is the basis for treatment of this condition. Endoscopic sinus surgery (ESS) is widely accepted as the surgical procedure of choice for treating CRS, which is refractory to conventional medical therapy as it promotes sinonasal airway patency and clears the sinuses while reducing the severity of the inflammation. Nevertheless, it is not always a simple and benign procedure and potential complications include postoperative severe bleeding, mucosal adhesions, infection, inflammation, and compromised surgical outcomes.[2]

Steroids are commonly used for managing CRS due to their potent anti-inflammatory properties. However, while oral steroids are effective, their use is associated with several adverse effects.[3] Therefore, topical steroids have been increasingly used due to their favorable safety profile and due to the fact that intranasal administration via various nasal sprays is very common and generally preferred both by patients and physicians. Intranasal steroids are considered a basic treatment modality of CRS therapy, providing high local concentrations of the drug while minimizing systemic exposure.[4] Mometasone furoate (MF) has been demonstrated to be effective in treating nasal inflammatory disorders.[5,6] It has been used in clinical practice for sinonasal indications for more than 20 years, and a significant body of literature has demonstrated its beneficial properties for such conditions. A systematic review by Passali et al. examined the effectiveness of MF nasal sprays in CRS.[5] MF was shown to be more effective than its competitors in terms of symptom control and safety profile. Furthermore, Meltzer et al. investigated the efficacy of MF versus antibiotics in treating CRS and showed that MF was significantly superior to amoxicillin in the treatment of this condition.[7] MF (Figure 1) is a highly lipophilic and poorly water-soluble drug with a relatively low risk of systemic absorption.[8]

Poor water solubility of drugs is one of the most significant problems in drug development. Insoluble drugs require

Received: January 9, 2020
Accepted: March 16, 2020
Published: March 25, 2020

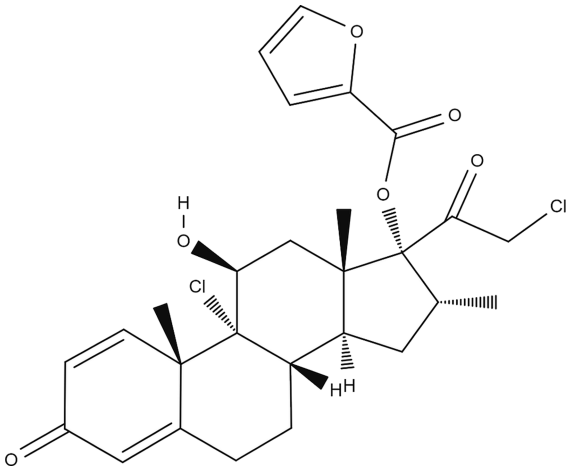

Figure 1. Chemical structure of mometasone furoate.

excipients to increase solubility, including surfactants, cosolvents, micellar solutions, complexing agents, and lipid formulations.[9] Unfortunately, the increased number of ingredients required to formulate the poorly water-soluble molecules may raise the potential for adverse effects.

Nanotechnology-based drug delivery can overcome certain anatomical, physiological, chemical, and clinical barriers associated with conventional dosage forms. Nanoparticles (NPs) are submicrometer particulate dispersions, or solid particles, that can deliver a variety of important therapeutic agents such as nucleic acids, peptides, and small hydrophobic and hydrophilic molecules to different biological systems. The potential advantages of NPs include improved drug solubility and stability, increased bioavailability at the targeted area, and prolonged duration of action by controlling the release rate. This can result in minimal adverse effects and a more convenient route of administration, leading to improved patient compliance and enhanced therapeutic outcome. Many types of nanotherapeutics have been designed and evaluated over the years (for example, based on liposomes, polymers, and micelles as carrier materials).[10] Among the carrier materials, the copolymer poly(lactic-*co*-glycolic acid) (PLGA) has a long history of use as a biomaterial due to its exceptional biocompatibility and biodegradability. The properties of molecular weight and biodegradation rate can be controlled over a wide range of values.[11] The hydrolyzed monomers are easily metabolized in the body via the Krebs cycle and eliminated as carbon dioxide and water. PLGA has been approved by the FDA for use in drug delivery systems due to its controlled and sustained release properties and biocompatibility with biological tissues and cells.[12]

Drug-loaded PLGA NPs are most commonly prepared by nanoprecipitation[13,14] and single or double emulsion solvent evaporation, in which various stabilizers and organic solvents are used and have a critical effect on physicochemical properties of NPs.[15,16] Furthermore, PLGA molecular weights, drug/polymer ratios, and nanoprecipitation conditions all affect the final properties of the NPs.[17−19] Solutol HS15 is a biocompatible nonionic surfactant with high stability and excellent solubilization ability of hydrophobic drugs. It is also characterized by increased mucosal permeability and altered drug pharmacokinetics.[20]

The only preparation of MF-loaded PLGA NPs found by the authors was conjugated with wheat germ agglutinin (WGA), reported by Surti et al. The preparation was carried out by an emulsion−solvent evaporation technique using polyvinyl alcohol (PVA) as a stabilizer.[21] Interestingly, there are no reports about the preparation and optimization of PLGA nanoparticles containing MF through the nanoprecipitation method using Solutol HS15 as a stabilizer. The aim of this study is to design and characterize PLGA NPs encapsulating MF for sustained drug release using nanoprecipitation. This may lead to improved therapeutic outcome and patient compliance.

2. EXPERIMENTAL SECTION

2.1. Materials. Mometasone furoate (MF) was purchased from Acros Organics (New Jersey, USA). PLGA-Purasorb PDLG 5010 (50:50) with an inherent viscosity midpoint of 1 dL/g was kindly donated by Corbion Purac (Gorinchem, the Netherlands). Solutol HS 15 (Macrogol 15 hydroxystearate) was kindly supplied by BASF (Ludwigshafen, Germany). Sodium dodecyl sulfate (SDS) was purchased from Biological Industries (Beit HaEmek, Israel). Acetone and methanol were purchased from Sigma-Aldrich (Rehovot, Israel). Spectra/Por Biotech 1.1 dialysis membranes with a molecular weight cutoff (MWCO) of 8000 Da were purchased from Spectrum Medical Industries (Houston, Texas, USA).

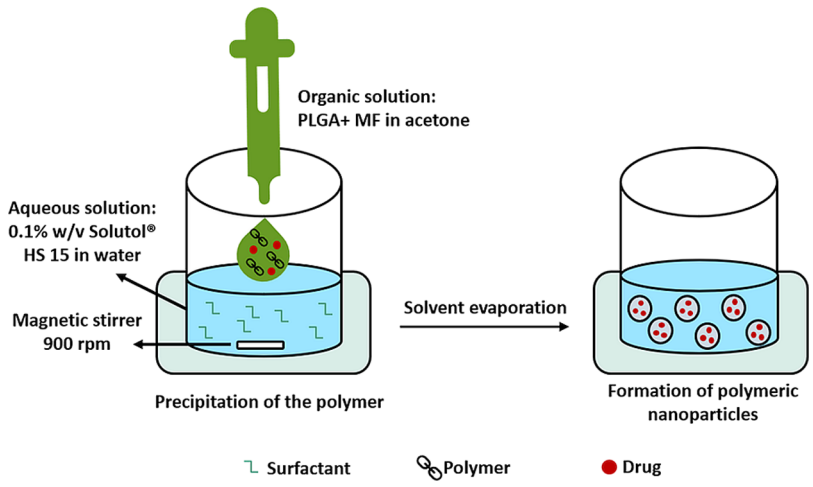

Figure 2. Schematic illustration of the preparation of MF NPs using the nanoprecipitation method.

https://dx.doi.org/10.1021/acsomega.0c00111
ACS Omega 2020, 5, 7432−7439

Table 1. Physicochemical Properties, Encapsulation Efficiency, and Drug Loading Content of MF NPs (n = 3, mean ± s.d.)

formulation	mean diameter (nm)	polydispersity index (PDI)	zeta potential (mV)	encapsulation efficiency (%)[a]	drug loading content (%)[b]
MF NPs	117 ± 13	0.26 ± 0.02	−32 ± 1.2	90 ± 2.1	22.4 ± 0.5

[a]Encapsulation efficiency (%) = (amount of drug in nanoparticles/amount of drug fed initially) × 100. [b]Drug loading content (%) = [amount of drug/(amount of drug + amount of polymer)] × 100.

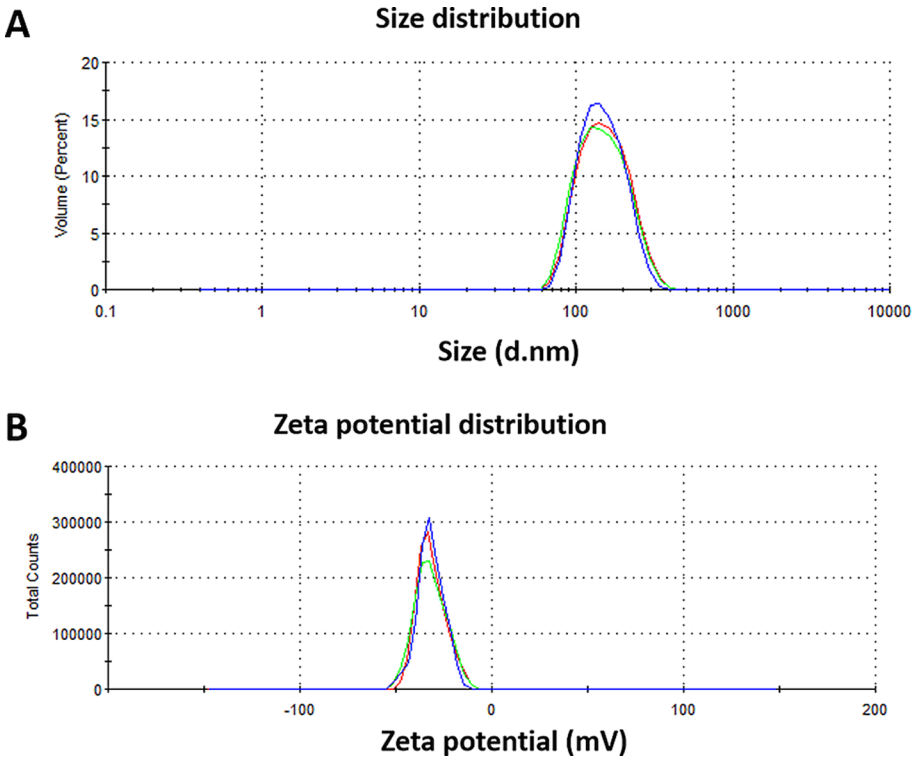

Figure 3. Representative DLS measurements for the (A) size and (B) zeta potential distribution of MF NPs.

2.2. Preparation of MF NPs. MF-loaded nanoparticles were prepared using the nanoprecipitation method[13] with modification. The organic phase, consisting of 2 mg of MF and 6 mg of PLGA in 1 mL of acetone, was rapidly poured into 2 mL of aqueous solution containing 0.1% (w/v) Solutol HS 15. The suspension was stirred at 900 rpm for 24 h to allow complete evaporation of the organic solvent, and the formulation volume was adjusted with water to 2 mL (Figure 2). Complete evaporation was confirmed by weighting the glass vial before addition of the organic phase and after the evaporation process. Then, the formulation was centrifuged for 1 min at 3000 rpm to discard debris. The supernatant was then transferred to a new tube for further investigation.

2.3. Physicochemical Characterization of MF NPs. Particle size distribution, polydispersity index (PDI), and zeta potential of NPs were characterized by dynamic light scattering (DLS) using Malvern's Zetasizer (Nano series, Nanos-ZS, U.K.) at 25 °C using water as a diluent.

2.4. Determination of Drug Encapsulation Efficiency. MF NPs were centrifuged for 30 min at 13,600 rpm to precipitate the NPs. The supernatant was discarded, and the sediment was dissolved in acetone. Methanol was then added to precipitate the polymer, followed by vortex and centrifugation for 1 min at 2000 rpm. Afterward, the supernatant containing the drug and organic solvents was transferred and evaporated. Methanol was then added to the residue, and the MF concentration was determined using a Biochrom UV−Vis spectrophotometer at a wavelength of 248 nm. The concentrations of the calibration curve ranged from 0 to 16 μg/mL (Figure S1).

2.5. Morphological Evaluation of MF NPs. Morphological evaluation of MF NPs was carried out using scanning electron microscopy (SEM) and scanning transmission electron microscopy (STEM) by an extreme high-resolution scanning electron microscope (XHR SEM) (model Magellan 400L, FEI, Germany). The samples were diluted with water and fixed on an SEM stub.

2.6. In Vitro Drug Release Studies. MF NPs containing 225 μg of MF were placed in dialysis bags with a molecular cut-off of 8000 Da. The dialysis bags were suspended in 50 mL of phosphate-buffered saline (PBS) containing 1% SDS (pH 7.4 and pH 6.4) and maintained at 37 °C (150 rpm). At predetermined time intervals, 1 mL of the release medium was discarded and replaced by an equal volume of fresh medium to maintain sink conditions. The concentration of MF was determined using UV−Vis at a wavelength of 248 nm. The concentrations of the calibration curves in PBS containing 1% SDS ranged from 0 to 17.5 μg/mL (Figure S2).

2.7. Kinetics of Drug Release. The data obtained from release studies were analyzed by different mathematical models to study the kinetics of the drug release from the prepared nanoparticles: Higuchi's model (cumulative percent of drug released vs $(\text{time})^{1/2}$), zero order (cumulative percent drug released vs time), first order (log cumulative percent of drug retained vs time), and the first 60% drug release fit in

https://dx.doi.org/10.1021/acsomega.0c00111
ACS Omega 2020, 5, 7432−7439

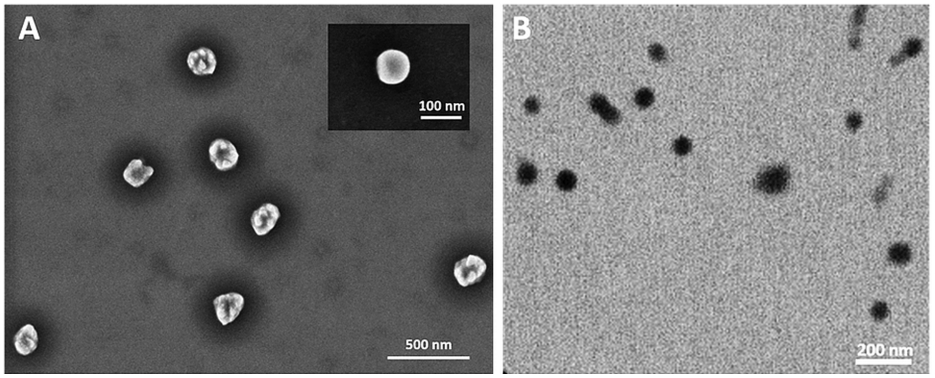

Figure 4. (A) SEM and (B) STEM images of the obtained MF NPs. The inset shows an amplified image of one nanoparticle.

Korsmeyer−Peppas model (log of cumulative percent of drug released vs log of time).[22]

2.8. Freeze-Drying of MF NPs. The MF NPs were lyophilized in the presence of two cryoprotectants, mannitol and sucrose, at three different concentrations: 4, 6, and 8% (w/v). After cryoprotectant dissolution in nanosuspension, samples were kept at −80 °C for at least 24 h prior to lyophilization. The lyophilized MF NPs were then reconstituted to the initial volume, and their physicochemical properties were evaluated.

3. RESULTS AND DISCUSSION

Topical steroids constitute first-line therapy in the medical management of CRS, a persistent inflammatory condition characterized by the accumulation of highly viscoelastic mucus in the sinuses. However, the clinical outcome of topical steroids is often limited, mainly due to the poor distribution to the nose and sinuses.[23] Localized drug delivery using NPs may facilitate consistent delivery to targeted sites, prolonged contact time, local elevated drug concentrations, reduced systemic adverse effects, and improved therapeutic outcome. NPs have been used in the respiratory system as drug vehicles capable of minimizing mucociliary clearance and avoiding phagocytosis by macrophages, consequently enhancing the drug absorption.[24]

Lai et al. reported that the estimated average pore size of CRS mucus was at least 150 ± 50 nm, and polymeric nanoparticles up to 200 nm in diameter were capable of readily penetrating highly viscoelastic CRS mucus.[25] Huang and Donovan found that amine-modified polystyrene nanoparticles that were smaller than 200 nm were transported across rabbit nasal respiratory epithelium by both paracellular and transcellular routes.[26] In this study, MF-loaded PLGA NPs were successfully prepared using the nanoprecipitation method with a mean particle size of 117 nm and a satisfactory polydispersity index (PDI) of 0.26 (Table 1 and Figure 3A) such that they should be able to easily penetrate the CRS mucus.

Zeta potential analysis is routinely used to determine the surface charge and stability of NPs. The zeta potential is an important parameter to evaluate colloidal dispersions. Values between −30 and + 30 mV indicate a tendency toward instability, aggregation, coagulation, or flocculation.[27] Negative zeta potential values of approximately −32 mV were obtained for MF NPs, indicating the stability of particles (Table 1 and Figure 3B). The zeta potential influences the ability of NPs to penetrate the mucosal layer where negative charges may facilitate penetration into the mucus layer.[28,29]

The drug encapsulation efficiency was 90 ± 2.1%, as determined by UV spectroscopy (Table 1). In a previous study, the MF encapsulation efficiency in PLGA NPs and WGA-conjugated PLGA NPs using an emulsion−solvent evaporation technique was 78 ± 5.5 and 60 ± 2.5%, respectively.[21] Moreover, the drug loading content was 22.4 ± 0.5% (w/w), where most of the existing nanomedicines usually do not reach values higher than 10% drug loading content.[30]

The morphology of MF NPs was investigated. Figure 4 shows the SEM and STEM images of the obtained NPs. The morphology of the nanocarriers was almost spherical for all the tested samples. The mean size of NPs was in agreement with that measured using DLS within experimental errors. Moreover, a size distribution was observed and could be explained by the polydispersity value found by DLS.

To evaluate the potential application of MF NPs for nasal delivery, the in vitro release of MF from PLGA NPs was examined in PBS (pH 6.4 and pH 7.4) containing 1% SDS to mimic the nasal mucosal microenvironment pH and physiological pH, respectively, at 37 °C for 7 days. The cumulative release curve of MF exhibited burst release initially followed by a sustained release phase, and the release was higher at lower pH, as expected[31] (Figure 5). The initial burst release of the drug can

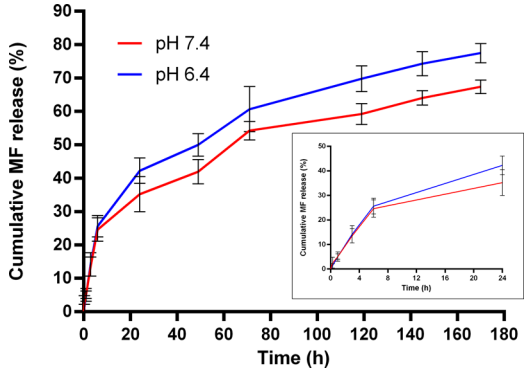

Figure 5. In vitro drug release of MF from MF NPs in PBS with 1% SDS (pH 7.4 and pH 6.4, 37 °C) at different time intervals. The inset shows the drug release profile over the initial 24 h. Values are the mean ± s.d. of three experiments.

occur if an appreciable amount is weakly bound or adsorbed to the relatively large surface of the NPs.[32] Similar findings were also reported by Gaonkar et al. using the exact polymer with a hydrophobic compound.[33]

Mathematical models are commonly used to determine the kinetics of drug release from drug delivery systems. The data obtained from in vitro release studies were fit to several models

https://dx.doi.org/10.1021/acsomega.0c00111
ACS Omega 2020, 5, 7432−7439

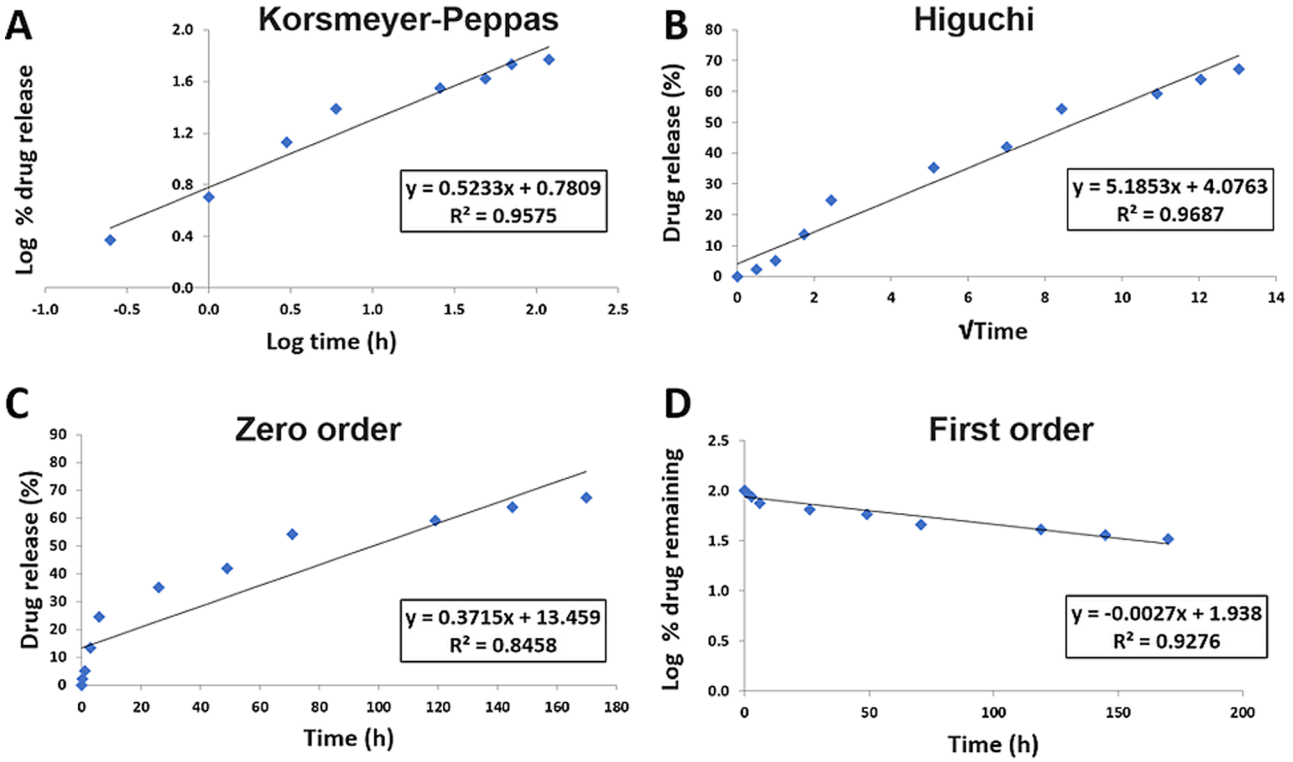

Figure 6. MF release from PLGA NPs at pH 7.4 fit to kinetic models. (A) Korsmeyer–Peppas, (B) Higuchi, (C) zero-order, and (D) first-order models.

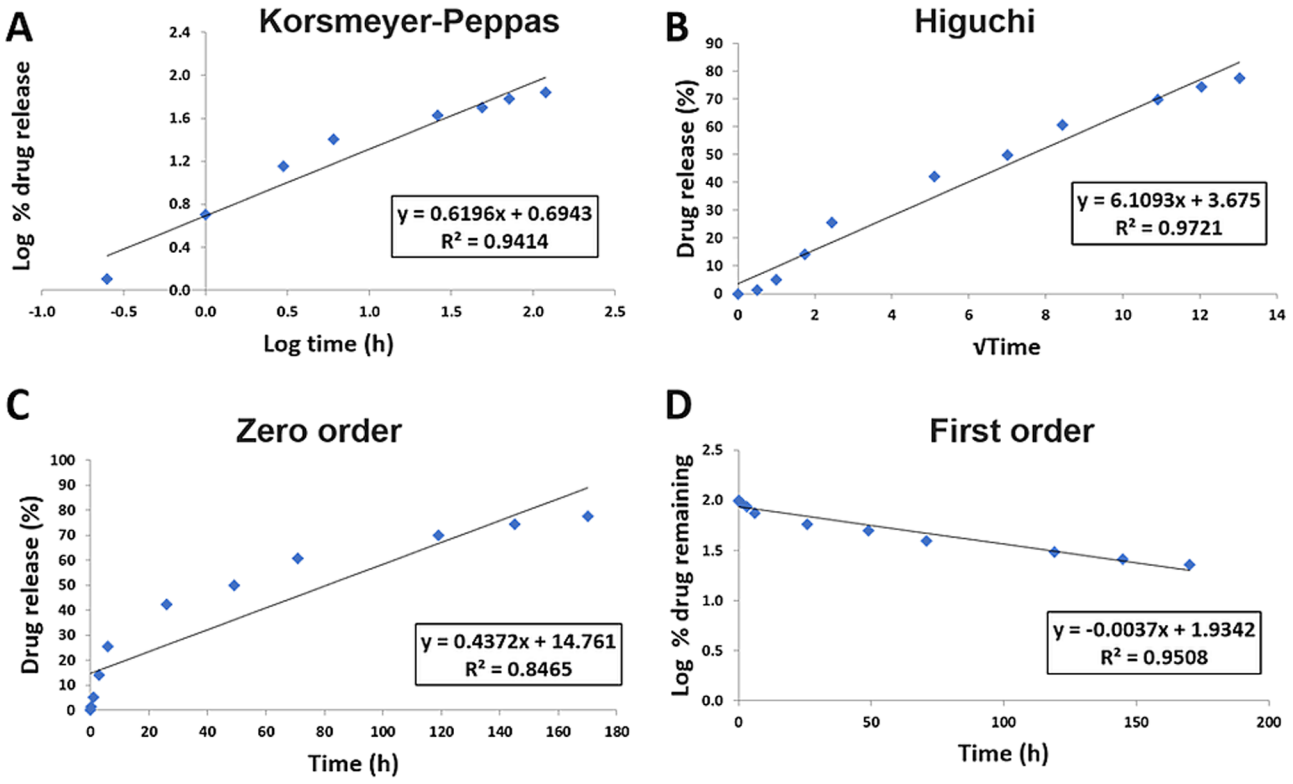

Figure 7. MF release from PLGA NPs at pH 6.4 fit to kinetic models. (A) Korsmeyer–Peppas, (B) Higuchi, (C) zero-order, and (D) first-order models.

to determine the mechanism of drug release from the prepared NPs (Figures 6 and 7). Higher R^2 values were observed in the first-order model relative to the zero-order model, revealing a concentration-dependent release. Under both pH conditions, MF NPs were found to have higher R^2 values for Higuchi's model, indicating that the release of MF from PLGA NPs is

https://dx.doi.org/10.1021/acsomega.0c00111
ACS Omega 2020, 5, 7432−7439

Table 2. Physicochemical Properties of MF NPs after Freeze-Drying Using Cryoprotectants at Different Concentrations (n = 3, mean ± s.d.)

cryoprotectant	concentration (% w/v)	mean diameter (nm)	PDI	zeta potential (mV)	S_f/S_i[a]
sucrose	4%	162 ± 12	0.44 ± 0.06	−32 ± 1	1.38
	6%	206 ± 7.6	0.45 ± 0.02	−39 ± 4	1.75
	8%	146 ± 17	0.43 ± 0.02	−30.4 ± 0.7	1.25
mannitol	4%	210 ± 31	0.39 ± 0.01	−32.3 ± 2.6	1.78
	6%	256 ± 2.2	0.42 ± 0.01	−36.5 ± 0.5	2.18
	8%	206 ± 4.5	0.36 ± 0.02	−31.3 ± 0.4	1.75

[a] S_f/S_i is the ratio of particle size after freeze-drying to particle size and before freeze-drying.

controlled by diffusion. However, Higuchi's model does not take into account the influence of swelling of the matrix upon hydration or erosion of the matrix.[34] However, high R^2 values were obtained for the Korsmeyer−Peppas model, in which the first 60% drug release data were fit. In this model, the value of the release exponent "n" characterizes the release mechanism of drug from the matrix system. Under both pH conditions, the obtained release exponents were $0.45 < n < 0.89$, suggesting that the release followed anomalous non-Fickian transport due to a combination of drug diffusion through the polymer, polymeric erosion, swelling, and degradation.[22,35] Since PLGA degradation is usually slow, the release of MF from PLGA NPs would depend chiefly on drug diffusion kinetics and the matrix swelling and erosion, as described by other works using hydrophobic drugs.[36,37] The timescale over which our delivery system was studied is shorter than the time during which PLGA undergoes degradation.[38−41]

Freeze-drying is a reliable method to maintain the stability of pharmaceutical products and to facilitate handling and storage.[42] As this process is highly stressful for NPs, cryoprotectants must be added before freezing to protect the NPs. The most favorable cryoprotectants for freeze-dried NPs are sugar derivatives.[43] Particle size analysis with the mean diameter ratio of NPs after and before freeze-drying (S_f/S_i) is the key determinant of formulation success. The NPs are assumed to be stable throughout the freeze-drying process if the ratio S_f/S_i is close to 1, with an upper limit of 2.[44−46] In the present study, sucrose and mannitol were used as cryoprotectants at different concentrations, and the physicochemical properties of MF NPs were measured by DLS after freeze-drying (Table 2). S_f/S_i ratios for MF NPs using different concentrations of sucrose and mannitol ranged from 1.25 to 1.78, with the exception of mannitol 6%, in which the S_f/S_i ratio was 2.18. The change in particle size distribution may result from the cryoprotectants' behavior during freeze-drying and their adsorption on the NP surface.[47] Additionally, the zeta potential values were in the range of −30.4 to −39.1 mV, indicating good stability of MF NPs after the freeze-drying process using 4−8% cryoprotectants.

The effect of cryoprotectants on MF release after the freeze-drying process was investigated on the system with 8% (w/v) cryoprotectant because it had the lowest S_f/S_i ratio observed. Figure 8 shows drug release rates under both pH conditions with cryoprotectants, where the extent of initial burst release decreased for all freeze-dried formulations and the release profiles were modified. At pH 7.4, NPs with sucrose and mannitol cryoprotectants showed a slight decrease in the release rate and cumulative percentage of MF released, in addition to the reduction in burst release. At pH 6.4, while a lower percentage of MF was initially released when sucrose and mannitol were added used, a significantly higher cumulative percentage of MF was obtained for sucrose within the tested

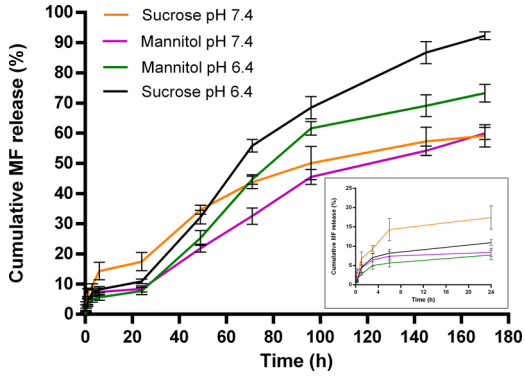

Figure 8. In vitro drug release of MF from MF NPs after freeze-drying using 8% (w/v) sucrose and mannitol in PBS with 1% SDS (pH 7.4 and pH 6.4, 37 °C) at different time intervals. The inset shows the drug release profile over the initial 24 h. Values are the mean ± s.d. of three experiments.

time period absolutely and in comparison to mannitol and MF NPs without a cryoprotectant. The NPs with mannitol cryoprotectant show a similar release profile at both pH values as without the cryoprotectant after the decrease in initial burst release.

The data obtained from in vitro release studies were fit by several models to determine the mechanism of drug release from the freeze-dried NPs (Table 3 and Figures S3−S6). The release

Table 3. Correlation Coefficient (R^2) Values of Various Release Kinetic Models in 1% SDS Buffers (pH 7.4 and pH 6.4) for Freeze-Dried MF NPs

	zero order	first order	Higuchi model	Korsmeyer−Peppas model	
cryoprotectant [8% (w/v)]	R^2	R^2	R^2	n	R^2
sucrose pH 7.4	0.907	0.955	0.984	0.57	0.934
sucrose pH 6.4	0.971	0.975	0.952	0.66	0.985
mannitol pH 7.4	0.975	0.988	0.950	0.46	0.953
mannitol pH 6.4	0.954	0.976	0.940	0.63	0.980

kinetics of MF from NPs after freeze-drying showed the best fit for first-order kinetics, and the release exponents obtained from Korsmeyer−Peppas model were $0.45 < n < 0.89$, suggesting that the release followed anomalous non-Fickian transport.

4. CONCLUSIONS

To the best of our knowledge, this is the first report of a preparation of PLGA NPs containing MF using the nanoprecipitation method. MF-loaded PLGA NPs were successfully prepared and exhibited adequate physicochemical properties as

https://dx.doi.org/10.1021/acsomega.0c00111
ACS Omega 2020, 5, 7432−7439

well as high drug encapsulation efficiency and loading content. The in vitro MF release from PLGA NPs under pH conditions mimicking the nasal mucosal microenvironment showed initial burst release followed by a sustained release phase. The kinetics of drug release followed anomalous non-Fickian transport, and the NPs could be lyophilized to give stable NPs with reduced initial burst release that could be advantageous for a final formulation. Local treatment of CRS with nasal MF NPs can be beneficial in decreasing the overall required dosage, in minimizing side effects, and in enhancing patient compliance. In conclusion, we expect that controlled release of MF using PLGA NPs will be a promising approach for improving the local treatment of CRS; hence, their potential for nasal delivery applications warrants further in vitro and in vivo investigations.

■ ASSOCIATED CONTENT

Supporting Information

The Supporting Information is available free of charge at https://pubs.acs.org/doi/10.1021/acsomega.0c00111.

Calibration curves of MF in methanol and 1% SDS PBS solution of pH 6.4 and pH 7.4 (Figures S1 and S2) and fitting of MF release from PLGA NPs after freeze-drying using cryoprotectants at pH 6.4 and pH 7.4 to kinetic models (Figures S3−S6) (PDF)

■ AUTHOR INFORMATION

Corresponding Author

Aiman Abu Ammar − *Department of Pharmaceutical Engineering, Azrieli College of Engineering Jerusalem, Jerusalem 9103501, Israel;* orcid.org/0000-0002-2556-3120; Email: aimanab@jce.ac.il, +972-2-6591835

Authors

Jumana Far − *Department of Pharmaceutical Engineering, Azrieli College of Engineering Jerusalem, Jerusalem 9103501, Israel*

Muhammad Abdel-Haq − *Department of Pharmaceutical Engineering, Azrieli College of Engineering Jerusalem, Jerusalem 9103501, Israel*

Maayan Gruber − *Department of Otolaryngology−Head and Neck Surgery, Galilee Medical Center, Nahariya 2210001, Israel; Faculty of Medicine in the Galilee, Bar-Ilan University, Safed 1311502, Israel*

Complete contact information is available at: https://pubs.acs.org/10.1021/acsomega.0c00111

Notes

The authors declare no competing financial interest.

■ ACKNOWLEDGMENTS

This research was funded by the Azrieli College of Engineering Jerusalem (A.A.A).

■ REFERENCES

(1) Benninger, M. S.; Ferguson, B. J.; Hadley, J. A.; Hamilos, D. L.; Jacobs, M.; Kennedy, D. W.; Lanza, D. C.; Marple, B. F.; Osguthorpe, J. D.; Stankiewicz, J. A.; et al. Adult Chronic Rhinosinusitis: Definitions, Diagnosis, Epidemiology, and Pathophysiology. *Otolaryngol.–Neck Surg.* **2003**, *129*, S1−S32.

(2) Asaka, D.; Nakayama, T.; Hama, T.; Okushi, T.; Matsuwaki, Y.; Yoshikawa, M.; Yanagi, K.; Moriyama, H.; Otori, N. Risk Factors for Complications of Endoscopic Sinus Surgery for Chronic Rhinosinusitis. *Am. J. Rhinol. Allergy* **2012**, *26*, 61−64.

(3) Poetker, D. M.; Reh, D. D. A Comprehensive Review of the Adverse Effects of Systemic Corticosteroids. *Otolaryngol. Clin. North Am.* **2010**, *43*, 753−768.

(4) Varshney, R.; Lee, J. T. Current Trends in Topical Therapies for Chronic Rhinosinusitis: Update and Literature Review. *Expert Opin. Drug Delivery* **2017**, *14*, 257−271.

(5) Passali, D.; Spinosi, M. C.; Crisanti, A.; Bellussi, L. M. Mometasone Furoate Nasal Spray: A Systematic Review. *Multidiscip. Respir. Med.* **2016**, *11*, 18.

(6) Berlucchi, M.; Pedruzzi, B. Intranasal Mometasone Furoate for Treatment of Allergic Rhinitis. *Clin. Med. Insights: Ther.* **2010**, *2*, CMT.S4767.

(7) Meltzer, E. O.; Gates, D.; Bachert, C. Mometasone Furoate Nasal Spray Increases the Number of Minimal-Symptom Days in Patients with Acute Rhinosinusitis. *Ann. Allergy, Asthma, Immunol.* **2012**, *108*, 275−279.

(8) Abu Ammar, A.; Gruber, M.; Martin, P.; Stern, O.; Jahshan, F.; Ertracht, O.; Sela, E.; Srouji, S.; Zussman, E. Local Delivery of Mometasone Furoate from an Eluting Endotracheal Tube. *J. Controlled Release* **2018**, *272*, 54−61.

(9) Bhakay, A.; Rahman, M.; Dave, R. N.; Bilgili, E. Bioavailability Enhancement of Poorly Water-Soluble Drugs via Nanocomposites: Formulation−Processing Aspects and Challenges. *Pharmaceutics* **2018**, *10*, 86.

(10) Patra, J. K.; Das, G.; Fraceto, L. F.; Campos, E. V. R.; Rodriguez-Torres, M. D. P.; Acosta-Torres, L. S.; Diaz-Torres, L. A.; Grillo, R.; Swamy, M. K.; Sharma, S.; et al. Nano Based Drug Delivery Systems: Recent Developments and Future Prospects. *J. Nanobiotechnol.* **2018**, *16*, 71.

(11) Sun, X.; Xu, C.; Wu, G.; Ye, Q.; Wang, C. Poly(Lactic-Co-Glycolic Acid): Applications and Future Prospects for Periodontal Tissue Regeneration. *Polymer* **2017**, *9*, 189.

(12) Swider, E.; Koshkina, O.; Tel, J.; Cruz, L. J.; de Vries, I. J. M.; Srinivas, M. Customizing Poly(Lactic-Co-Glycolic Acid) Particles for Biomedical Applications. *Acta Biomater.* **2018**, *73*, 38−51.

(13) Abu Ammar, A.; Nasereddin, A.; Ereqat, S.; Dan-Goor, M.; Jaffe, C. L.; Zussman, E.; Abdeen, Z. Amphotericin B-Loaded Nanoparticles for Local Treatment of Cutaneous Leishmaniasis. *Drug Delivery Transl. Res.* **2019**, *9*, 76−84.

(14) Abu Ammar, A.; Raveendran, R.; Gibson, D.; Nassar, T.; Benita, S. A Lipophilic Pt(IV) Oxaliplatin Derivative Enhances Antitumor Activity. *J. Med. Chem.* **2016**, *59*, 9035−9046.

(15) Sharma, S.; Parmar, A.; Kori, S.; Sandhir, R. PLGA-Based Nanoparticles: A New Paradigm in Biomedical Applications. *TrAC, Trends Anal. Chem.* **2016**, *80*, 30−40.

(16) Iqbal, M.; Zafar, N.; Fessi, H.; Elaissari, A. Double Emulsion Solvent Evaporation Techniques Used for Drug Encapsulation. *Int. J. Pharm.* **2015**, *496*, 173−190.

(17) Hernández-Giottonini, K. Y.; Rodríguez-Córdova, R. J.; Gutiérrez-Valenzuela, C. A.; Peñuñuri-Miranda, O.; Zavala-Rivera, P.; Guerrero-Germán, P.; Lucero-Acuña, A. PLGA Nanoparticle Preparations by Emulsification and Nanoprecipitation Techniques: Effects of Formulation Parameters. *RSC Adv.* **2020**, *10*, 4218−4231.

(18) Huang, W.; Zhang, C. Tuning the Size of Poly(Lactic-Co-Glycolic Acid) (PLGA) Nanoparticles Fabricated by Nanoprecipitation. *Biotechnol. J.* **2018**, *13*, 1700203.

(19) Martínez Rivas, C. J.; Tarhini, M.; Badri, W.; Miladi, K.; Greige-Gerges, H.; Nazari, Q. A.; Galindo Rodríguez, S. A.; Román, R. A.; Fessi, H.; Elaissari, A. Nanoprecipitation Process: From Encapsulation to Drug Delivery. *Int. J. Pharm.* **2017**, *532*, 66−81.

(20) Younes, N. F.; Abdel-Halim, S. A.; Elassasy, A. I. Solutol HS15 Based Binary Mixed Micelles with Penetration Enhancers for Augmented Corneal Delivery of Sertaconazole Nitrate: Optimization, in Vitro, Ex Vivo and in Vivo Characterization. *Drug Delivery* **2018**, *25*, 1706−1717.

(21) Surti, N.; Naik, S.; Bagchi, T.; Dwarkanath, B. S.; Misra, A. Intracellular Delivery of Nanoparticles of an Antiasthmatic Drug. *AAPS PharmSciTech* **2008**, *9*, 217−223.

(22) Dash, S.; Murthy, P. N.; Nath, L.; Chowdhury, P. Kinetic Modeling on Drug Release from Controlled Drug Delivery Systems. *Acta Pol. Pharm.* **2010**, *67*, 217−223.
(23) Kumar, A.; Pandey, A. N.; Jain, S. K. Nasal-Nanotechnology: Revolution for Efficient Therapeutics Delivery. *Drug Delivery* **2016**, *23*, 671−683.
(24) Ghadiri, M.; Young, P. M.; Traini, D. Strategies to Enhance Drug Absorption via Nasal and Pulmonary Routes. *Pharmaceutics* **2019**, *11*, 113.
(25) Lai, S. K.; Suk, J. S.; Pace, A.; Wang, Y.-Y.; Yang, M.; Mert, O.; Chen, J.; Kim, J.; Hanes, J. Drug Carrier Nanoparticles That Penetrate Human Chronic Rhinosinusitis Mucus. *Biomaterials* **2011**, *32*, 6285−6290.
(26) Huang, Y.; Donovan, M. Microsphere Transport Pathways in the Rabbit Nasal Mucosa. *Int. J. Pharm. Adv.* **1996**, *1*, 298−309.
(27) Crucho, C. I. C.; Barros, M. T. Polymeric Nanoparticles: A Study on the Preparation Variables and Characterization Methods. *Mater. Sci. Eng., C* **2017**, *80*, 771−784.
(28) Dünnhaupt, S.; Kammona, O.; Waldner, C.; Kiparissides, C.; Bernkop-Schnürch, A. Nano-Carrier Systems: Strategies to Overcome the Mucus Gel Barrier. *Eur. J. Pharm. Biopharm.* **2015**, *96*, 447−453.
(29) Müller, C.; Perera, G.; König, V.; Bernkop-Schnürch, A. Development and in Vivo Evaluation of Papain-Functionalized Nanoparticles. *Eur. J. Pharm. Biopharm.* **2014**, *87*, 125−131.
(30) Shen, S.; Wu, Y.; Liu, Y.; Wu, D. High Drug-Loading Nanomedicines: Progress, Current Status, and Prospects. *Int. J. Nanomed.* **2017**, *12*, 4085−4109.
(31) Li, B.; Xu, H.; Yao, M.; Xie, M.; Shen, H.; Shen, S.; Wang, X.; Jin, Y. Bypassing Multidrug Resistance in Human Breast Cancer Cells with Lipid/Polymer Particle Assemblies. *Int. J. Nanomed.* **2012**, *7*, 187.
(32) Venkatasubbu, G. D.; Ramasamy, S.; Avadhani, G. S.; Ramakrishnan, V.; Kumar, J. Surface Modification and Paclitaxel Drug Delivery of Folic Acid Modified Polyethylene Glycol Functionalized Hydroxyapatite Nanoparticles. *Powder Technol.* **2013**, *235*, 437−442.
(33) Gaonkar, R. H.; Ganguly, S.; Dewanjee, S.; Sinha, S.; Gupta, A.; Ganguly, S.; Chattopadhyay, D.; Chatterjee Debnath, M. Garcinol Loaded Vitamin E TPGS Emulsified PLGA Nanoparticles: Preparation, Physicochemical Characterization, in Vitro and in Vivo Studies. *Sci. Rep.* **2017**, *7*, 530.
(34) Siepmann, J.; Peppas, N. A. Higuchi Equation: Derivation, Applications, Use and Misuse. *Int. J. Pharm.* **2011**, *418*, 6−12.
(35) Mircioiu, C.; Voicu, V.; Anuta, V.; Tudose, A.; Celia, C.; Paolino, D.; Fresta, M.; Sandulovici, R.; Mircioiu, I. Mathematical Modeling of Release Kinetics from Supramolecular Drug Delivery Systems. *Pharmaceutics* **2019**, *11*, 140.
(36) Keum, C.-G.; Noh, Y.-W.; Baek, J.-S.; Lim, J.-H.; Hwang, C.-J.; Na, Y.-G.; Shin, S.-C.; Cho, C.-W. Practical Preparation Procedures for Docetaxel-Loaded Nanoparticles Using Polylactic Acid-Co-Glycolic Acid. *Int. J. Nanomed.* **2011**, *6*, 2225−2234.
(37) Takeuchi, I.; Tomoda, K.; Hamano, A.; Makino, K. Effects of Physicochemical Properties of Poly(Lactide-Co-Glycolide) on Drug Release Behavior of Hydrophobic Drug-Loaded Nanoparticles. *Colloids Surf., A* **2017**, *520*, 771−778.
(38) Ansary, R. H.; Awang, M. B.; Rahman, M. M. Biodegradable Poly(D,L-Lactic-Co-Glycolic Acid)-Based Micro/Nanoparticles for Sustained Release of Protein Drugs - A Review. *Trop. J. Pharm. Res.* **2014**, *13*, 1179.
(39) Huang, C. L.; Steele, T. W. J.; Widjaja, E.; Boey, F. Y. C.; Venkatraman, S. S.; Loo, J. S. C. The Influence of Additives in Modulating Drug Delivery and Degradation of PLGA Thin Films. *NPG Asia Mater.* **2013**, *5*, e54.
(40) Fredenberg, S.; Wahlgren, M.; Reslow, M.; Axelsson, A. The Mechanisms of Drug Release in Poly(Lactic-Co-Glycolic Acid)-Based Drug Delivery Systems—A Review. *Int. J. Pharm.* **2011**, *415*, 34−52.
(41) Dunne, M.; Corrigan, O. I.; Ramtoola, Z. Influence of Particle Size and Dissolution Conditions on the Degradation Properties of Polylactide-Co-Glycolide Particles. *Biomaterials* **2000**, *21*, 1659−1668.
(42) Emami, F.; Vatanara, A.; Park, E. J.; Na, D. H. Drying Technologies for the Stability and Bioavailability of Biopharmaceuticals. *Pharmaceutics* **2018**, *10*, 131.
(43) Holzer, M.; Vogel, V.; Mäntele, W.; Schwartz, D.; Haase, W.; Langer, K. Physico-Chemical Characterisation of PLGA Nanoparticles after Freeze-Drying and Storage. *Eur. J. Pharm. Biopharm.* **2009**, *72*, 428−437.
(44) Pawar, H.; Surapaneni, S. K.; Tikoo, K.; Singh, C.; Burman, R.; Gill, M. S.; Suresh, S. Folic Acid Functionalized Long-Circulating Co-Encapsulated Docetaxel and Curcumin Solid Lipid Nanoparticles: In Vitro Evaluation, Pharmacokinetic and Biodistribution in Rats. *Drug Delivery* **2016**, *23*, 1453−1468.
(45) Moretton, M. A.; Chiappetta, D. A.; Sosnik, A. Cryoprotection-Lyophilization and Physical Stabilization of Rifampicin-Loaded Flower-like Polymeric Micelles. *J. R. Soc., Interface* **2011**, *9*, 487−502.
(46) Saez, A.; Guzmán, M.; Molpeceres, J.; Aberturas, M. R. Freeze-Drying of Polycaprolactone and Poly(D,L-Lactic-Glycolic) Nanoparticles Induce Minor Particle Size Changes Affecting the Oral Pharmacokinetics of Loaded Drugs. *Eur. J. Pharm. Biopharm.* **2000**, *50*, 379−387.
(47) Fonte, P.; Soares, S.; Costa, A.; Andrade, J. C.; Seabra, V.; Reis, S.; Sarmento, B. Effect of Cryoprotectants on the Porosity and Stability of Insulin-Loaded PLGA Nanoparticles after Freeze-Drying. *Biomatter* **2012**, *2*, 329−339.

https://dx.doi.org/10.1021/acsomega.0c00111
ACS Omega 2020, 5, 7432−7439